

**A review of the design and clinical evaluation of the
ShefStim array-based functional electrical stimulation
system**

KENNEY, Laurence, HELLER, Ben <<http://orcid.org/0000-0003-0805-8170>>, BARKER, Anthony T., REEVES, Mark L., HEALEY, Jamie, GOOD, Timothy R., COOPER, Glen, SHA, Ning, PRENTON, Sarah, LIU, Anmin and HOWARD, David

Available from Sheffield Hallam University Research Archive (SHURA) at:

<http://shura.shu.ac.uk/13301/>

This document is the author deposited version. You are advised to consult the publisher's version if you wish to cite from it.

Published version

KENNEY, Laurence, HELLER, Ben, BARKER, Anthony T., REEVES, Mark L., HEALEY, Jamie, GOOD, Timothy R., COOPER, Glen, SHA, Ning, PRENTON, Sarah, LIU, Anmin and HOWARD, David (2016). A review of the design and clinical evaluation of the ShefStim array-based functional electrical stimulation system. *Medical Engineering & Physics*, 38 (11), 1159-1165.

Copyright and re-use policy

See <http://shura.shu.ac.uk/information.html>

A review of the design and clinical evaluation of the ShefStim array-based functional electrical stimulation system.

Laurence P. Kenney*¹, Ben W. Heller², Anthony T. Barker³, Mark L. Reeves³, Jamie Healey³, Timothy R. Good³, Glen Cooper^{1,4}, Ning Sha¹, Sarah Prenton^{1,5}, Anmin Liu¹, David Howard¹

¹Centre for Health Sciences Research, University of Salford, Salford M6 6PU, U.K.

² Centre for Sports Engineering Research, Sheffield Hallam University, Sheffield S1 1WB, U.K.

³ Department of Medical Physics and Clinical Engineering, Royal Hallamshire Hospital, Sheffield S10 2JF U.K.

⁴School of Mechanical, Aerospace and Civil Engineering, University of Manchester, Manchester, M13 9PL, U.K.

⁵ Division of Health and Rehabilitation, University of Huddersfield, Huddersfield HD1 3DH, U.K.

* Corresponding author: email - l.p.j.kenney@salford.ac.uk; tel 0161295 2289

Abstract: Functional electrical stimulation has been shown to be a safe and effective means of correcting foot drop of central neurological origin. Current surface-based devices typically consist of a single channel stimulator, a sensor for determining gait phase and a cuff, within which is housed the anode and cathode. The cuff-mounted electrode design reduces the likelihood of large errors in electrode placement, but the user is still fully responsible for selecting the correct stimulation level each time the system is donned. Researchers have investigated different approaches to automating aspects of setup and/or use, including recent promising work based on iterative learning techniques. This paper reports on the design and clinical evaluation of an electrode array-based FES system for the correction of drop foot, ShefStim. The paper reviews the design process from proof of concept lab-based study, through modelling of the array geometry and interface layer to array search algorithm development. Finally, the paper summarises two clinical studies involving patients with drop foot. The results suggest that the ShefStim system with automated setup produces results which are comparable with clinician setup of conventional systems. Further, the final study demonstrated that patients can use the system without clinical supervision. When used unsupervised, setup time was 14 minutes (9 minutes for automated search plus 5 minutes for donning the equipment), although this figure could be reduced significantly with relatively minor changes to the design.

1. INTRODUCTION

Functional electrical stimulation has been shown to be a safe and effective means of correcting foot drop of central neurological origin [1-3]. Surface-based devices typically stimulate via a cathode placed over the common peroneal nerve immediately distal to where it bifurcates into the deep and superficial branches, and an anode placed over tibialis anterior. Appropriate levels of stimulation delivered via accurately placed electrodes should result in suitably weighted recruitment of the two nerve branches, leading to a useful and safe foot response during the swing phase of walking (dorsiflexion with a small degree of eversion). However, in certain individuals even very small electrode positioning errors can lead to a poor foot response. Indeed, a 1999 survey of users of drop foot stimulators reported over 40% of respondents finding electrode positioning problematic [4]. Some current systems such as the WalkAide (Innovative Neurotronics Inc., Austin, Texas, USA) embed electrodes in a cuff, worn below the knee (the reader is referred to [5] for a recent review of current systems). Such an approach greatly reduces the likelihood of large errors in electrode placement, but the user is still fully responsible for selecting the correct stimulation level each time the system is donned. Interestingly, despite improvements in both stimulator designs and patient education, two recent studies demonstrated that when patients set up their stimulators without clinician support, the resultant foot response is often less than optimal [6, 7].

One approach to the challenge of stimulator setup is to implant the electrodes on the nerve(s), thereby removing the electrode placement problem from the user [8, 9]. However, an invasive approach carries risks and the implantable devices and surgical costs remain relatively expensive. As a result, a number of groups have been investigating the possibility of automating the surface-based drop foot setup process through a two-channel stimulation approach to software steering of the foot [10-12], or electrode array-based approaches [13-18]. Both approaches feature a 'setup space' which can be automatically searched, either through replacing single electrode(s) with one or two arrays of discrete electrodes, or by allowing modulation of pulse waveform. Both approaches also use measurement of foot orientation, usually derived from foot-worn inertial sensors, to guide the search.

Elsaify proposed an automatic array element search algorithm, but using array elements with separate gel layers (a matrix of small single electrodes) [14]. More recently, Valtin [17] demonstrated an array search algorithm that

53 takes roughly two minutes using two flexible PCB electrode arrays (one over the nerve and one over Tibialis
54 Anterior), each interfaced with a continuous, high-resistivity hydrogel layer. However, in contrast to the work
55 presented here, only preliminary results with a healthy subject were presented. In the most recent work, Seel
56 reported on a system using a foot-mounted inertial sensor to adjust the steering based on realtime measurements
57 of the foot orientation[11]. The system uses only two electrodes and, in laboratory studies with stroke participants,
58 demonstrates convergence on a suitable foot response within one or two strides. However, studies of the system
59 outside of the laboratory setting have yet to be published.

60 In this paper we expand on a recent conference paper [19] to report on the design, development and demonstration
61 of a system for automated setup of drop foot FES (ShefStim). The paper extends the conference paper by
62 presenting the model used to define the initial electrode array geometry design (section 2) and provides discussion
63 of the merits and limitations of ShefStim compared with alternative systems. The ShefStim design concept was
64 proposed by Heller in 2003 [20]. For this study the Department of Medical Physics at Sheffield Teaching Hospitals
65 initially developed a ‘proof-of-concept’ multi-electrode stimulator, which could simultaneously stimulate any
66 manually-selected subset out of a conveniently sized, 8 by 8 rectangular array of metal electrodes. The subset of
67 activated electrodes is termed a virtual electrode (VE). In order to develop this concept into a clinically usable
68 system for automated setup a series of design problems needed to be solved. The first problem was the electrode
69 array design; the second problem was the development of an array search algorithm. The remaining part of the
70 paper summarises the results from two studies of the ShefStim involving people with drop foot of central
71 neurological origin.

72

73 2. DESIGN OF THE ELECTRODE ARRAY

74 For clinical applications a moderately electrically conductive hydrogel interface between the electrodes and skin
75 provides the benefits of hydration of, and adhesion to, the skin. However, in array applications a continuous
76 hydrogel layer also introduces the issue of spatial selectivity loss due to transverse currents in the hydrogel. Spatial
77 selectivity is defined as the ability to activate discrete groups of nerve fibres in a localised region without
78 stimulating nerve fibres in neighbouring regions.

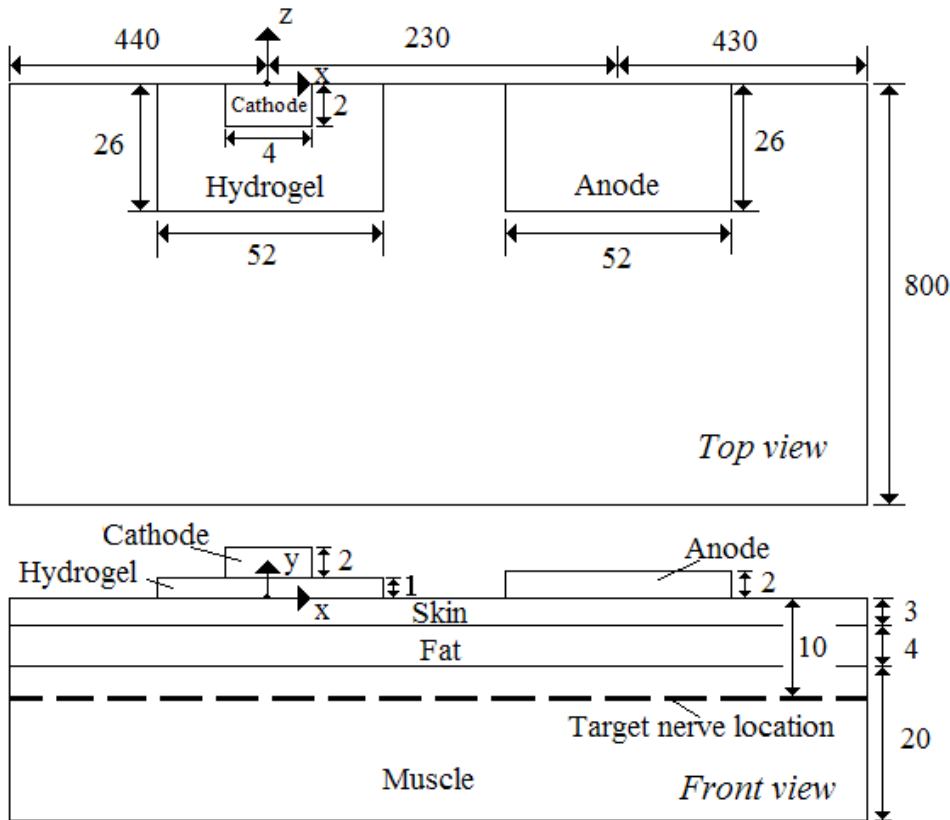
79 In order to achieve a satisfactory degree of spatial selectivity, it was necessary to identify an appropriate electrode
80 geometry and interface layer properties. Two finite-element models were therefore developed to investigate the
81 effects of electrode geometry and hydrogel layer properties on spatial selectivity, characterised in our model by
82 the activation area (see below). Model 1 was developed to explore the effects of hydrogel resistivity and electrode
83 size on activation area under a single cathode electrode and; Model 2 extended Model 1 through the addition of
84 electrodes surrounding the cathode, to allow investigation of activation area under a multi-electrode array. The
85 results of the second model, together with practical constraints imposed by the stimulator, led to the array
86 geometry and interface layer properties used in part 3 of this paper.

87 *Model 1*

88 Figure 1 shows the 3D finite-element model, developed using ANSYS Multiphysics (Version 10.0, Ansys, Inc,
89 Canonsburg, PA, USA) to predict the effects of electrode geometry and hydrogel properties on electric field
90 distribution in the underlying tissue [21]. The model represents a cathode, an anode, a hydrogel layer, skin, fat
91 and muscle. The skin, fat and muscle were modelled as flat, extended layers, whose thicknesses were based on
92 their anatomical dimensions. As bone has much higher resistivity than the other media, it was assumed to be non-
93 conductive volume underlying the muscle, and hence was represented as the lower boundary of the model.
94 Structures of smaller dimension, such as hair follicles or blood vessels, were not explicitly modelled, as their
95 influence on stimulation at the depth of the motor nerve branches could be considered negligible.

96 Appropriate electrical conductivity properties were assigned to the elements, based on values from Duck [22]
97 (Table 1). Although the skin’s capacitance cannot normally be neglected, the skin in the model was assumed to

98 be hydrated due to intimate contact with the hydrogel layer. Hence capacitive effects were not included in this
 99 model.



100
 101 *Figure 1: Schematic of the geometry of the selectivity FE model (not to scale) (dimensions in mm)*

102
 103 *Table 1: Model parameters*

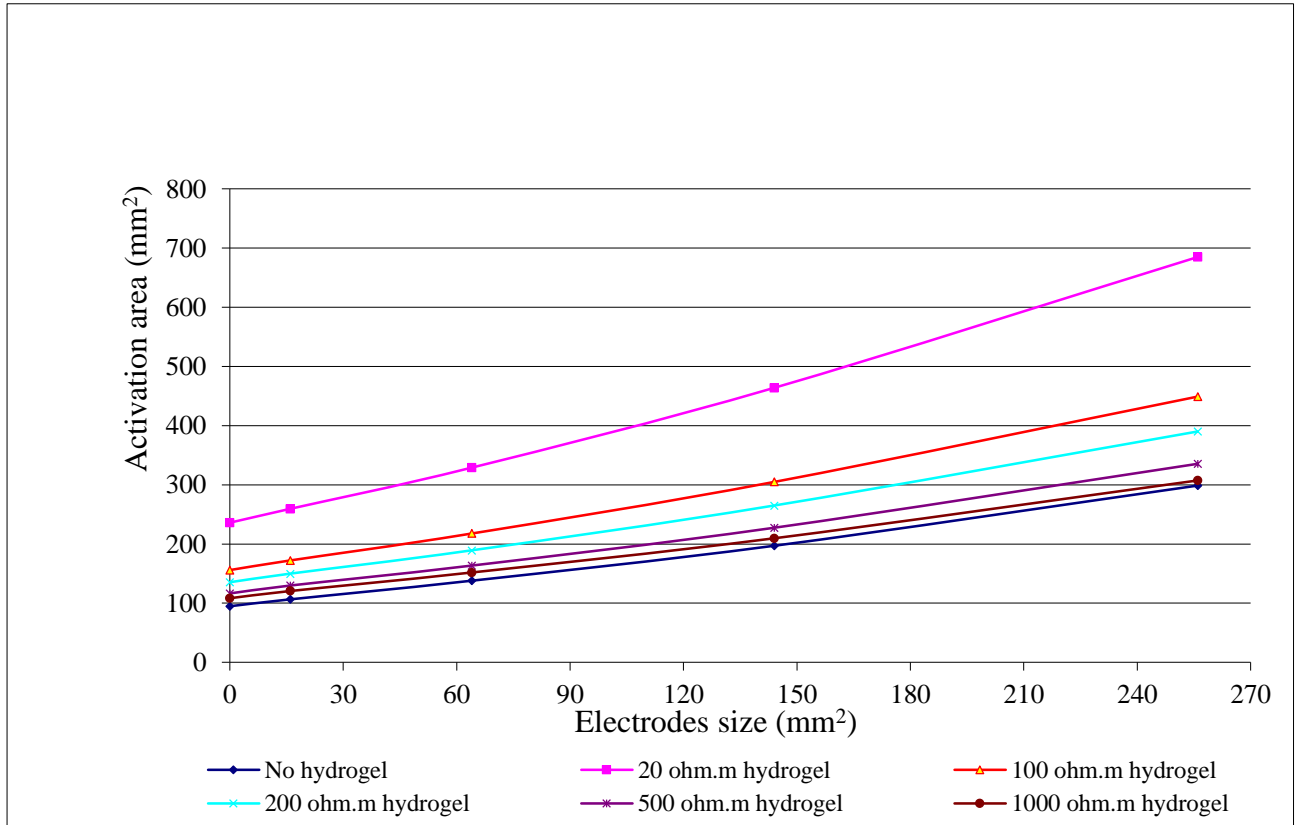
Biological tissues and materials	Resistivity (Ωm)
Bone	7×10^4
Muscle	2 in X and Z directions
	4 in Y direction
Fat	62.5
Skin (hydrated)	833
Hydrogel	Model variable
Cathode and Anode	1.5×10^{-8}

104
 105 The calculation of whether a point in the model was deemed to be stimulated was based on the stimulation function
 106 [23]. To explore spatial selectivity we first defined a stimulus pool to be a volume over which the value of the
 107 stimulation function exceeds a threshold at which action potentials in a nerve fibre are generated. The maximum
 108 stimulation function always appears in the stimulus pool centre, just underneath the cathode, and the amplitude of
 109 the stimulation function decreases from the centre to the edge of the stimulus pool. Although the value of the
 110 maximum stimulation function varies between models, it can always be scaled to the same value by changing the
 111 input current, and this scaling does not change the shape or size of the stimulus pool. Contours may be defined
 112 which connect points in the model with identical stimulation function values (expressed as a percentage of the
 113 maximum) and the 50% contour was selected to represent the boundary of the stimulus pool for the results
 114 presented here. The 50% contour choice was somewhat arbitrary, but avoided problems which would be
 115 associated with choice of a contour near 100% or 0% of maximum stimulation function (all contours converge to
 116 a point at 100% of maximum stimulation function and contours enclose infinitely large areas at 0%) As the
 117 electrical properties of the tissue were uniform, the current density distribution was symmetric along the plane
 118 normal to the skin surface and along the centres of the cathode and the anode. This symmetry allowed a study to

119 be performed on a half model. To represent the location of the nerve, we defined a plane representing the
 120 anatomical depth of the target nerve (10mm). The intersection of the stimulus pool with the plane defined an area;
 121 the smaller the area, the more focused is the stimulation and thus the better the spatial selectivity. Therefore, the
 122 area of the stimulus contour associated with 50% of maximal stimulation was used as the metric of spatial
 123 selectivity.

124 To explore the combined effect of hydrogel resistivity and electrode size on selectivity, a series of simulations
 125 were run with square electrodes from infinitely small (a point) to 16mm×16mm with a range of interface layers.
 126 The first simulation considered the no interface layer case; subsequent simulations varied the 1mm thick hydrogel
 127 layer resistivity from 20Ωm to 1000Ωm. The results are shown in Figure 1.

128



129
 130 *Figure 2: The effects of electrode size on activation area for a range of hydrogel resistivities.*

131

132

133 Figure 1 shows that there is a minimum limit to activation area of approximately 100mm² at 10mm depth, and
 134 that spatial selectivity becomes poorer (activation area increases) with increasing size of electrode and decreasing
 135 resistivity. When the resistivity reaches 500Ωm or greater, the spatial selectivity is similar to that of the model
 136 without the hydrogel sheet.

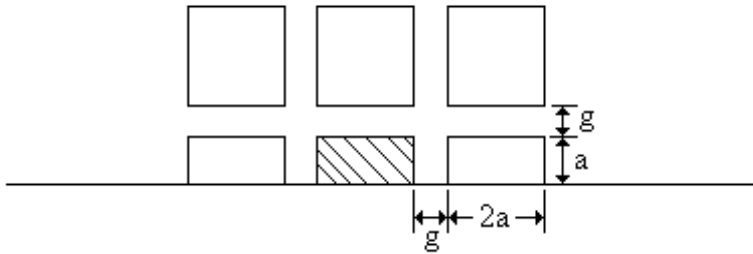
137 *Model 2*

138 Model 1 had shown that the introduction of a 1 mm hydrogel interface layer did not significantly degrade
 139 selectivity providing the hydrogel resistivity was at least 500Ωm. However, the model did not account for the
 140 presence of neighbouring electrodes which would surround an electrode in the array. The presence of these
 141 electrodes will lead to a decrease in selectivity compared with the single electrode condition, as current can flow
 142 from activated electrodes across inter-electrode gaps and into adjacent non-activated electrodes. These effects
 143 would be modulated by the size of the inter-electrode gap and hydrogel properties. Therefore, Model 1 was used
 144 as the basis for a new model (Model 2) to enable the electrode array design to be finalised.

145 It was assumed that the magnitude of reduction in selectivity due to current passing across the inter-electrode gaps
 146 would be dominated by electrodes immediately surrounding any given electrode in the array. Hence, Model 1 was

147 extended to include eight more electrodes surrounding the original cathode electrode (Figure 2)¹. The interface
 148 between the electrode array and the skin was a sheet of hydrogel. The initial geometry of Model 2 was informed
 149 by previous pilot experimental work carried out as part of a Master’s research project, demonstrating the viability
 150 of using a 70mm x70mm electrode array consisting of 64 electrodes (arranged in an 8x8 format)[24].

151
 152



153 surrounding electrodes the stimulating electrode

154 *Figure 3: Model 2. The electrode gap (g) is the edge-to-edge distance between any two neighbouring electrodes in the array;*
 155 *2a is the dimension of each square electrode*

156 As the feasibility work suggested maintaining an overall array size of approximately 70mm x 70mm , we fixed
 157 the centre-to-centre spacing of electrodes in the model to be 9mm ($2a + g = 9$, see Figure 2). Five different gap
 158 sizes were modelled (Table 1) and for each of these, four commercial hydrogel sheets were modelled (Table 2).
 159 The set of hydrogel properties were informed not only by the results of Model 1, but also by earlier experimental
 160 work [25, 26] which provided further evidence to support the use of a thin, high-resistivity hydrogel layer between
 161 the electrode and skin.

162 *Table 2: Electrode gap and size evaluated in the FE model, and resultant overall electrode array size*

Electrode gap (mm)	Electrode size (mm)	Electrode array size (mm)
1	8×8	71×71
2	7×7	70×70
3	6×6	69×69
4	5×5	68×68
5	4×4	67×67

163

164 *Table 3: Hydrogel materials represented in the model. Note that the different sheet thicknesses modelled were chosen to*
 165 *represent the sheet thicknesses provided by the manufacturers.*

Hydrogel (abbreviation)	Approx thickness (mm)	Resisitvity at 1.67kHz (Ωm)
AG703, Axelgaard manufacture Co., Ltd. Fallbrook, CA. USA (Hydrogel 703)	0.9	55
AG803, Axelgaard manufacture Co., Ltd. Fallbrook, CA. USA (Hydrogel 803)	0.9	206
SRBZAB-05SB, Sekisui Plastics, Co., Ltd. Tokyo, Japan (Hydrogel ST)	0.5	1363
AG, AG3AM03M-P10W05, Sekisui Plastics, Co., Ltd. Tokyo, Japan (Hydrogel AG)	0.3	25185

¹ Note, as per Model 1, a half model was developed to take advantage of symmetry.

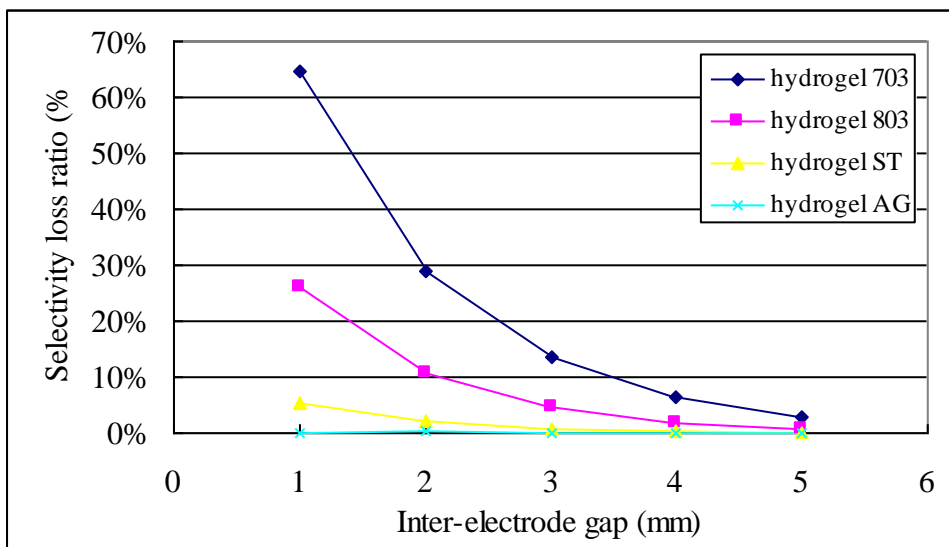
166
167
168
169
170

In order to quantify the effects of the surrounding electrodes on selectivity, two versions of each model were run. In the first version, the surrounding electrodes were not represented and in the second, the surrounding electrodes were represented. The selectivity loss resulting from the introduction of surrounding electrodes was quantified by a selectivity loss ratio, defined in equation 1.

171
$$Selectivity_loss_ratio = \frac{A_2 - A_1}{A_1} \times 100\% \quad (1)$$

172 Where, A_1 is the activation area of the model without surrounding electrode and A_2 is the activation area of the
173 model with surrounding electrode
174

175 Figure 3 shows the selectivity loss ratio due to the surrounding electrodes calculated for each combination of
176 hydrogel interface layer and inter-electrode gap.
177



178
179 *Figure 3: Selectivity loss ratios with different hydrogels*

180 The results suggested that for hydrogels ST and AG an electrode gap between 1mm and 5mm will result in an
181 acceptably low selectivity loss (defined as less than 10%) in the presence of the surrounding electrodes. From a
182 manufacturing perspective, an inter-electrode gap of less than 2mm would make it very difficult to route the tracks
183 between electrodes, so a 2mm inter-electrode gap was chosen. A final practical test demonstrated that our
184 stimulator (200V drive voltage) could not drive the specified 8mA per channel when using the more resistive of
185 the two most promising materials (hydrogel AG) and hence hydrogel ST was selected.

186 3. FEASIBILITY STUDY OF ELECTRODE ARRAY SEARCH STRATEGY

187 Section 3 described the design of an 8 x 8 electrode array interfaced to the skin via a thin high-resistivity hydrogel
188 layer. The next design problem was the development of a quick, reliable method of searching the set of all possible
189 stimulation electrodes to find the optimal virtual electrode. In this section we report on two methods for searching
190 the array used to identify appropriate virtual electrodes and their associated stimulation levels, which extended
191 the work of Elsaify et al. [14]. In the first part of the work, we apply a slowly ramped stimulation through each
192 virtual electrode while continuously monitoring the orientation of the foot relative to the leg. These data allow
193 identification of electrode sets that, when appropriately stimulated, result in acceptable foot movement. The
194 ramped stimulation results were used to investigate whether it is possible to reduce the search space through
195 prediction of the location of the best subset of these electrodes based only on the response of the foot to short
196 bursts of stimulation (twitch stimulation). We investigated use of a cost function to rank the response to short
197 bursts of stimulation and examine whether this ranking may be used to isolate smaller groups of electrodes that
198 contain one or all of the best subset of electrodes identified in the slow ramped stimulation search.

199 For brevity, here we only report on the search for appropriate single VEs. Additional work to identify suitable
200 pairs of VEs is reported elsewhere [27]. Ethical approval for the study was granted by the University of Salford's

201 Research Governance and Ethics committee (RGE06/102). Twelve healthy subjects were recruited from within
202 the University and a full set of results were obtained for ten (9 male) subjects (median 30 years)².

203 The stimulation system consisted of a constant current portable 64 channel stimulator designed and built by the
204 Medical Engineering section of Sheffield Teaching Hospitals NHS Foundation Trust (size: 155 mm × 95 mm ×
205 33 mm), an 8×8 electrode array, described in section 2 and a 50×50 mm square conventional hydrogel electrode
206 (PALS® Platinum electrode, Axelgaard Manufacturing Co. Ltd.). The charge-balanced asymmetrical biphasic
207 stimulus pulses were software controllable via a graphical user interface, with the pulse width fixed at 300 μs, and
208 the frequency at 35 Hz. Stimulation intensity through each electrode was software controlled and measured by an
209 analogue to digital converter built-in to the stimulator itself. During the experiment, groups of 2×2 electrodes were
210 activated simultaneously (the minimum number required to elicit adequate contractions, providing a total current
211 of up to 32 mA), and act as a virtual electrode.
212

213 A 5-camera Qualisys motion capture system (Proreflex, Qualisys AB, Sweden) was used to record foot movement
214 at 100Hz and the motion data were transferred to and simultaneously analysed in Visual3D (Visual3D™, C-
215 Motion Inc, USA). Hence the foot movement was captured, and ankle angles in sagittal, coronal and transverse
216 planes were displayed in real-time. Synchronisation between the stimulator and the motion capture system was
217 achieved using a data acquisition device via the stimulator control program. An electrically-isolated button was
218 included to allow the user to stop stimulation at any stage in the experiment.

219 The experiment started with measurement of the neutral foot orientation for the subject while standing upright.
220 He/she was then asked to sit in a chair and their right lower leg was strapped in the brackets to keep the shank in
221 a consistent pose throughout. The stimulator and electrodes were then donned. The subject was then asked to
222 maintain their sitting posture and relax the foot in a natural (dropped) position throughout the experiments. As the
223 analysis of data did not dictate the order in which the tests were conducted, the foot twitch experiment was
224 conducted first to reduce fatigue. However, here they are explained in reverse order for clarity.

225 Prior to beginning the slow ramped stimulation experiment a user-defined maximal current was identified. We
226 assumed that sensation would be most acute over bony prominences and hence at the start of the experiment
227 increased stimulation over these sites until a user-defined maximum was reached and the value noted. Next,
228 current through each VE in turn was ramped from zero to the user-defined maximal current over 10 seconds. The
229 twitch stimulation part of the experiment involved six different bursts of stimulation (1 and 4 pulses/burst, at 3
230 different levels of stimulation (16, 24 and 32mA) being applied in turn through each of the 49 VEs. Ankle angles
231 together with time-synchronised current data for each of the different electrodes were recorded for both
232 experiments.
233

234 The target for foot orientation was defined as dorsiflexion at or above neutral, and inversion/eversion within -1SD
235 of the previously reported healthy subject mean foot orientation at heel strike [28]. All VEs which, when
236 stimulated over the 10 second period, resulted in the foot reaching the target foot orientation were identified and
237 the set of electrodes satisfying these criteria were labelled Set A.
238

239 When sitting relaxed in the chair the subject's foot was typically plantarflexed and inverted, compared with its
240 neutral position. Hence, it was assumed that a twitch response that moved the foot towards dorsiflexion and
241 eversion was desirable. A cost function was defined which used the maximum value of dorsiflexion and inversion
242 angles observed during the twitch response
243

$$244 \text{ Cost} = -2 \cdot \text{Dorsi} + \text{Inver}$$

245 Where *Dorsi* is the peak dorsiflexion angle (in degrees) measured during stimulation relative to the relaxed
246 position. Dorsiflexion is positive and plantarflexion is negative. *Inver* is the peak inversion angle (in degrees)
247 measured during stimulation relative to the relaxed position. Inversion is positive and eversion is negative. A
248 weighting factor of 2 was applied to the dorsiflexion angle to reflect its relative importance compared to
249 inversion/eversion.
250

251 This cost function was used to rank the foot responses to each of the different twitch stimulation bursts applied to
252 each of the VEs. The cost function, which was applied to the positive peak value of dorsiflexion and inversion,
253 maximizes dorsiflexion and minimizes inversion. The VE with the lowest cost was ranked 1st and each of the
254 remaining 48 VEs were then assigned a rank based on their cost. To identify how well the cost function could be
255 used to predict membership of Set A (the set of VEs which, when stimulated resulted in the foot reaching the

² Two subjects could only tolerate 12.8 mA and 16 mA respectively, which was insufficient to produce target dorsiflexion when applied through any of the virtual electrodes electrodes during the slowly ramped stimulation

256 target foot orientation) two metrics were derived. First, how far down the ranking it was necessary to go to include
 257 all of the members of Set A, defined as Rank_all ; second, how far down the ranking it was necessary to go to
 258 include any member of Set A, defined as Rank_any.
 259

260 In 9 out of the 10 subjects to complete the slow ramped stimulation study, at least 1 VE was identified which,
 261 when stimulated, produced the target foot response. The maximum number of acceptable VEs found for any
 262 individual subject was 4 (out of 49) and the minimum was 0.

263 The results of the twitch stimulation analysis for the 9 subjects are shown in Table 4. Note that stimulation at
 264 16mA produced no or minimal response.

265

266 *Table 4: Rank_any and Rank_all for different twitch stimuli*

	1 pulse @ 32mA	4 pulses @32mA	1 pulse @ 24mA	4 pulses @ 24mA
Rank_all Median (range)	5 (1-33)	4 (1-41)	11 (2-40)	8 (2-41)
Rank_any Median (range)	2 (1-19)	3 (1-15)	6 (1-15)	4 (1-29)

267

268 Although there was significant inter-subject variability, the results showed that in most cases by using a cost
 269 function to rank responses to twitch stimulation it was possible to identify a much smaller set of electrodes
 270 containing one, or all of Set A. For example, using a 4 pulse burst of stimulation at 32mA, a suitable electrode
 271 was identified in all cases within the first 15 of the responses ranked according to the slow ramped stimulation
 272 results. The data suggested therefore there could be advantage to using a twitch stimulation consisting of multiple
 273 pulses at high currents and a two stage search strategy was worth further investigation.

274 4. FIRST LAB-BASED DEMONSTRATION OF SHEFSTIM

275 Further development work on both the stimulator and the search algorithm was carried out over the period 2009-
 276 11 resulting in the first demonstration of an array-based FES system with automated setup for the correction of
 277 drop foot. The study is reported in detail elsewhere [6], so in this paper, we focus on the improvements made to
 278 the stimulator hardware and implementation of the search algorithm, and provide an overview of the laboratory-
 279 based study involving subjects with drop foot.

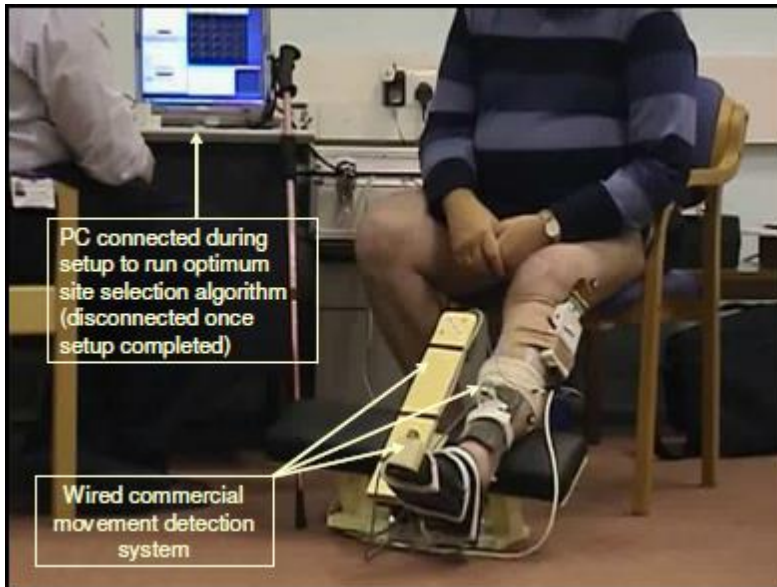
280 4.1 Stimulator

281 Further stimulator development led to a new design weighing 200 g with a volume of 211cc (130 mm x 65 mm x
 282 25 mm). During automated setup the stimulator was controlled via an isolated serial link by a program running
 283 on an external computer, the participant's leg was held in a brace, with the knee extended and foot movement was
 284 measured using an electromagnetic position and orientation sensor (Patriot, Polhemus Inc, Vermont) (Figure 4).
 285 For walking trials the setup parameters were downloaded and the stimulator disconnected from the computer,
 286 enabling it to function as a standalone drop foot stimulator being triggered using a foot switch.

287 4.2 Search algorithm

288 The work described in section 4 had been based on the use of a 2 x 2 VE. Following further pilot work it was
 289 found that a 4 x 4 VE still provided satisfactory resolution over foot response, but reduced sensation compared to
 290 a 2x2 arrangement and increased robustness to tissue movement during gait. The move to a 4 x 4 VE also served
 291 to reduce the array search space by a factor of ~2, compared with the original approach (25 VEs to be searched
 292 rather than 49).

293 As described in section 4, we had already demonstrated the potential to use the response of the foot to short bursts
 294 of stimulation as a means of homing in on promising VEs. However, further work was needed to develop a
 295 clinically usable search algorithm. In the final system a three phase search strategy was implemented.



296
297

Figure 4: Setup of ShefStim

298 In phase one the level of stimulation at which the foot first responds is determined. Short bursts of stimulation are
 299 applied to each of the 25 virtual electrodes, a process taking about 2.5 seconds. The amplitude is automatically
 300 titrated until the threshold for repeatable foot movement, irrespective of direction, is determined. This threshold
 301 amplitude is used as the base for searches in subsequent phases. In phase two (twitch response), the algorithm
 302 searches for candidate stimulation sites, using twitches rather than tetanic contractions to speed-up search time
 303 and reduce sensation. Four pulses of stimulation are applied to each electrode in turn. The foot response is
 304 monitored for short periods after each stimulation, if there is a detectable response it is added to the list of
 305 candidate sites. Again the current is automatically adjusted until between 4 and 12 sites are found or the maximum
 306 current limit is reached. These sites are ranked in order of sensitivity using a cost function based on the angular
 307 displacement. The first two stages therefore allowed for rapid identification of the most sensitive VEs.

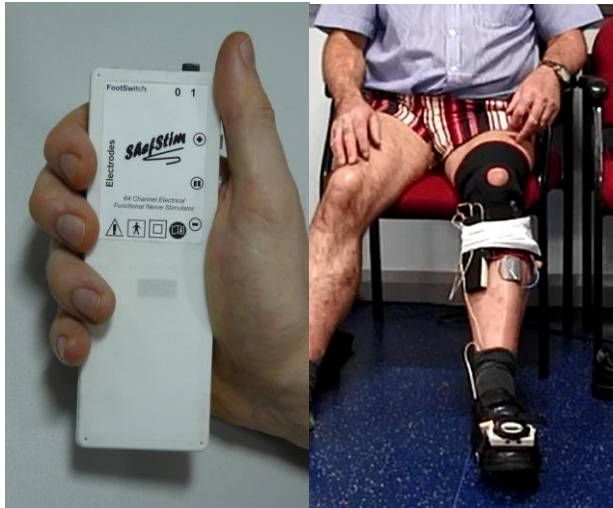
308 In phase three (tetanic testing), up to 8 of the sites identified in phase two were tested in rank order with an
 309 increasing stimulation intensity. Stimulation began at the level identified in phase two and incremented in steps
 310 until one of the following conditions were met: either plantarflexion was corrected to neutral dorsiflexion; or
 311 current reaching twice the starting value; or 150% of starting value with no movement detected; or motion
 312 saturation was detected. The algorithm included safeguards if unexpected movements occurred, enabling the
 313 system to temporarily wait if a leg spasm was detected or to pause the search process if repeated non-stimulated
 314 leg movement was detected. Once all the candidate sites were assessed, they were given a score based on a three-
 315 part cost function, designed to penalise solutions resulting in plantarflexion, excessive inversion or eversion, and
 316 high current. If at any point during this phase the user found a site uncomfortable the clinician was able to skip
 317 that site. Once the tetanic testing phase was complete the first-ranked site was activated and, after initial testing
 318 of the site while sitting, the user then walked using the stimulator: If the foot response or stimulation sensation
 319 was not satisfactory it could be manually changed to an alternative site the ranking list. Finally, stimulus pulse
 320 width could be adjusted by the user, if necessary, to fine-tune the magnitude of foot response.

321 **4.3 Laboratory-based clinical study**

322 Ten participants with drop foot due to stroke (ages 53–71 years) and 11 due to MS (ages 40–80 years) were
 323 recruited to test the system. Each participant walked twice over 10 m under each of four conditions; a). using their
 324 own stimulator setup by themselves; b) using their own stimulator set up by a clinician, c). using ShefStim with
 325 automated setup, and d). no stimulation. Outcome measures were walking speed, foot angle at initial contact and
 326 the Borg Rating of Perceived Exertion. As described in Heller et al [6], the results showed that when setup using
 327 ShefStim subjects' walking speed, dorsiflexion and frontal plane ankle angle at initial contact were all broadly
 328 comparable with clinician setup and, apart from walking speed, better than patient setup. The study demonstrated
 329 for the first time that fully automated setup of an array stimulator is feasible in a population with drop foot of
 330 central origin.

331 **5. FIRST TAKE-HOME STUDY OF SHEFSTIM**

332 A final iteration of the stimulator design resulted in the CE- marked ShefStim system shown below.



333
334 *Figure 5: ShefStim stimulator (left) being used by a subject during setup (right)*

335
336 The ShefStim stimulator measures 142mm x 50mm x 14mm (volume 99cc) and weighs 125 g (including
337 batteries). In contrast to the earlier versions of the system, it includes a combined foot angle sensor and remote
338 control device, and setup does not involve holding the leg in a brace (Figure 5). The remote control device is
339 placed on the foot during set up and wirelessly provides triaxial accelerometer inputs to the search algorithm
340 described in the previous section. Users are provided with an attachment, based on an iPod holder, which could
341 be slipped onto the shoe prior to setup. Guidance is provided to the users on the correct mounting of the remote
342 control on the shoe and the importance of aligning the ShefStim box with the long axis of the leg. Once setup is
343 completed, the foot angle sensor device serves as a remote control with which the user can pause stimulation,
344 adjust intensity or receive audible error messages. Stimulation timing during gait is controlled using a
345 conventional footswitch, located under the heel of the shoe. Integrating the foot angle sensor into the system
346 enabled the stimulator to carry out the automated setup routine without requiring input from any external sensors
347 or connection to a PC, making it suitable for use in the home environment.

348 In the final clinical study seven subjects with drop foot (3 subjects with MS, 3 with stroke and 1 with traumatic
349 brain injury) used ShefStim over a 2 week period. The reader is referred to [7] for the experimental protocol and
350 full results. Log data showed that all subjects were able to setup the stimulator outside of the laboratory
351 environment without technical support. Automated setup time averaged 9 minutes, plus 5 minutes to don the
352 equipment. Despite the challenges associated with unsupervised use, including the need for users to correctly align
353 the ShefStim, placed in a pocket of a leg-mounted sleeve, and the remote on their shoe, speed and foot response
354 with ShefStim, evaluated in a gait laboratory at the end of the 2 week period showed results comparable with the
355 previous study by Heller [6]. The study demonstrated, for the first time, that array-based automated setup FES
356 system for foot-drop can be successfully used without technical support outside of the laboratory environment.

357 6. DISCUSSION AND CONCLUSIONS

358 The work presented in this paper describes the evolution of the ShefStim design from initial concept in 2003 to
359 evaluation of the CE-marked system by people with stroke in their own homes. A number of issues are worth
360 discussing before conclusions are drawn on the revisions needed to be made to the design.

361 In section 2 we introduced two models used for the identification of electrode array geometry. The activation area
362 is similar in concept to the measure used by Kuhn et al [29], who based their measure of selectivity on an activation
363 volume. As our model assumes the nerve depth to be known (at 10mm in this case), the cross-sectional area of
364 the stimulation pool at 10mm is the measure of the selectivity of stimulation. The larger this area is, the less
365 selective the array stimulation is (i.e. the worse the ability to selectively stimulate neural structures). There are a
366 number of limitations with the model, including the prismatic geometry and assumptions regarding the nerve
367 depth, which undoubtedly varies significantly between subjects. Further, in contrast to Kuhn et al. [29], we did
368 not experimentally validate the model. However, the array geometry and hydrogel properties derived using the
369 model proved to be similar to the array design successfully used in the final take-home study.

370 Although the ShefStim stimulator has been CE marked, there remain a small number of barriers to clinical uptake.
371 By far the most significant of these is that sweat ingress to the hydrogel electrode interface layer leads to a
372 significant drop in its resistivity and an inevitable decay in focality and stimulation efficiency with wear time

373 [30]. These effects limit use of a given array to around one day of continuous wear. In the final study of ShefStim
374 [7] we were able to provide participants with sufficient arrays to use a fresh hydrogel layer each day. However,
375 the cost of such an approach is high and not a realistic solution in clinical practice. To address this we are exploring
376 alternative solutions, including the use of dry electrodes (see, for example [31]). Other minor product development
377 issues remain, including the development of an improved garment to house the stimulator on the leg and minor
378 improvements to the firmware, all of which may be easily resolved. We believe that these improvements would
379 lead to a significant reduction in setup time, as recorded in our final (unsupervised) study [7].

380 In conclusion, this paper has described the complete design, development and evaluation of an array-based FES
381 system with automated setup for the correction of drop foot. The results demonstrate that an array-based stimulator
382 with automated setup is a viable alternative to a conventional surface stimulator, or an implanted stimulator, for
383 the correction of drop foot. Longer term clinical exploitation of ShefStim is dependent on identifying an
384 acceptable alternative to the high-resistivity hydrogel electrode-skin interface layer.

385 **Acknowledgements**

386 This is a summary of independent research funded by the National Institute for Health Research (NIHR) under its
387 Invention for Innovation (i4i) Programme (grant ref HTD480), UK Overseas Research Studentship and Sheffield
388 Hospitals Charitable Trust. The views expressed are those of the author(s) and not necessarily those of the NHS,
389 the NIHR or the Department of Health, or other funding bodies.

390
391
392

393 [1] NICE. Functional electrical stimulation for drop foot of central neurological origin.
394 National Institute for Clinical Excellence; 2009. p. 2.

395 [2] Bosch PR, Harris JE, Wing K, American Congress of Rehabilitation Medicine Stroke
396 Movement Interventions S. Review of therapeutic electrical stimulation for dorsiflexion assist
397 and orthotic substitution from the American Congress of Rehabilitation Medicine stroke
398 movement interventions subcommittee. *Arch Phys Med Rehabil.* 2014;95:390-6.

399 [3] Roche A, Laighin G, Coote S. Surface-applied functional electrical stimulation for orthotic
400 and therapeutic treatment of drop-foot after stroke -- a systematic review. *Physical Therapy*
401 *Reviews.* 2009;14:63-80.

402 [4] Taylor PN, Burridge JH, Dunkerley AL, Lamb A, Wood DE, Norton JA, et al. Patients'
403 perceptions of the Odstock Dropped Foot Stimulator (ODFS). *Clin Rehabil.* 1999;13:439-46.

404 [5] Melo PL, Silva MT, Martins JM, Newman DJ. Technical developments of functional
405 electrical stimulation to correct drop foot: sensing, actuation and control strategies. *Clin*
406 *Biomech (Bristol, Avon).* 2015;30:101-13.

407 [6] Heller BW, Clarke AJ, Good TR, Healey TJ, Nair S, Pratt EJ, et al. Automated setup of
408 functional electrical stimulation for drop foot using a novel 64 channel prototype stimulator
409 and electrode array: results from a gait-lab based study. *Med Eng Phys.* 2013;35:74-81.

410 [7] Prenton S, Kenney LP, Stapleton C, Cooper G, Reeves ML, Heller BW, et al. Feasibility
411 study of a take-home array-based functional electrical stimulation system with automated setup
412 for current functional electrical stimulation users with foot-drop. *Arch Phys Med Rehabil.*
413 2014;95:1870-7.

414 [8] Burridge JH, Haugland M, Larsen B, Pickering RM, Svaneborg N, Iversen HK, et al. Phase
415 II trial to evaluate the ActiGait implanted drop-foot stimulator in established hemiplegia. *J*
416 *Rehabil Med.* 2007;39:212-8.

417 [9] Kottink AI, Hermens HJ, Nene AV, Tenniglo MJ, van der Aa HE, Buschman HP, et al. A
418 randomized controlled trial of an implantable 2-channel peroneal nerve stimulator on walking
419 speed and activity in poststroke hemiplegia. *Arch Phys Med Rehabil.* 2007;88:971-8.

420 [10] Merson E, Swain I, Taylor P, Cobb J. Two-channel stimulation for the correction of drop
421 foot. 5th Conference of IFESS UK & Ireland. Sheffield, UK2015.

422 [11] Seel T, Werner C, Raisch J, Schauer T. Iterative learning control of a drop foot
423 neuroprosthesis - Generating physiological foot motion in paretic gait by automatic feedback
424 control. *Control Eng Pract.* 2016;48:87-97.

425 [12] Seel T, Valtin M, Werner C, Schauer T. Multivariable Control of Foot Motion During
426 Gait by Peroneal Nerve Stimulation via two Skin Electrodes. 9th IFAC Symposium on
427 Biological and Medical Systems. Berlin, Germany2015.

428 [13] Whitlock T, Peasgood W, Fry M, Bateman A, Jones R. Self-optimising electrode arrays.
429 5th IPEM Clinical Functional Electrical Stimulation Meeting. Salisbury1997.

430 [14] Elsaify E, Fothergill J, Peasgood W. A portable FES system incorporating an electrode
431 array and feedback sensors. 8th Vienna International workshop functional electrical
432 stimulation. Vienna, Austria2004.

433 [15] Hernandez JD. Development and Evaluation of a Surface Array Based System to Assist
434 Electrode Positioning in FES for Drop Foot: University of Surrey; 2009.

435 [16] Kuhn A, Keller T, Micera S, Morari M. Array electrode design for transcutaneous
436 electrical stimulation: a simulation study. *Med Eng Phys.* 2009;31:945-51.

437 [17] Valtin M, Steel T, Raisch J, Schauer T. Iterative learning control of drop foot stimulation
438 with array electrodes for selective activation. 19th World Congress IFAC. Cape Town, South
439 Africa2014.

440 [18] Hernandez MD. Development and evaluation of a surface array based system to assist
441 electrode positioning in FES for drop foot: University of Surrey; 2009.

442 [19] Kenney L, Heller B, Barker AT, Reeves M, Healey J, Good T, et al. The Design,
443 Development and Evaluation of an Array-Based FES System with Automated Setup for the
444 Correction of Drop Foot. 9th IFAC Symposium on Biological and Medical System. Berlin,
445 Germany2015.

446 [20] Heller B, Barker AT, Sha N, Newman J, Harron E. Improved control of ankle movement
447 using an array of mini-electrodes. FES User Day Conference. Birmingham, U.K.2003.

448 [21] Sha N, Heller BW, Barker AT. 3D modelling of a hydrogel sheet - electrode array
449 combination for surface functional electrical stimulation. Proceedings of the 9th Annual
450 Conference of IFESS. Bournemouth, UK2004. p. 431-3.

451 [22] Duck FA. Physical properties of tissue : a comprehensive reference book. London:
452 Academic Press; 1990.

453 [23] Rattay F. Analysis of models for external stimulation of axons. *IEEE Trans Biomed Eng.*
454 1986;33:974-7.

455 [24] Sha N. Development of a steerable electrode array for functional electrical stimulation:
456 Sheffield University; 2003.

457 [25] Sha N, Kenney LP, Heller BW, Barker AT, Howard D, Wang W. The effect of the
458 impedance of a thin hydrogel electrode on sensation during functional electrical stimulation.
459 *Med Eng Phys.* 2008;30:739-46.

460 [26] Sha N, Kenney LP, Heller BW, Barker AT, Howard D, Moatamedi M. A finite element
461 model to identify electrode influence on current distribution in the skin. *Artif Organs.*
462 2008;32:639-43.

463 [27] Sha N. A surface electrode array-based system for functional electrical stimulation:
464 University of Salford; 2009.

465 [28] Woodburn J, Helliwell PS, Barker S. Three-dimensional kinematics at the ankle joint
466 complex in rheumatoid arthritis patients with painful valgus deformity of the rearfoot.
467 *Rheumatology (Oxford, England).* 2002;41:1406-12.

468 [29] Kuhn A, Keller T, Lawrence M, Morari M. The influence of electrode size on selectivity
469 and comfort in transcutaneous electrical stimulation of the forearm. *IEEE Trans Neural Syst*
470 *Rehabil Eng.* 2010;18:255-62.

471 [30] Cooper G, Barker AT, Heller BW, Good T, Kenney LP, Howard D. The use of hydrogel
472 as an electrode-skin interface for electrode array FES applications. *Med Eng Phys.*
473 2011;33:967-72.

474 [31] Yang K, Freeman C, Torah R, Beeby S, Tudor J. Screen printed fabric electrode array for
475 wearable functional electrical stimulation. *Sensor Actuat a-Phys.* 2014;213:108-15.
476